

A Neural Representation Framework with LLM-Driven Spatial Reasoning for Open-Vocabulary 3D Visual Grounding

Zhenyang Liu
lzyzjhz@163.com
Fudan University, Shanghai
Innovation Institute
Shanghai, China

Sixiao Zheng
sxzheng18@fudan.edu.cn
Fudan University, Shanghai
Innovation Institute
Shanghai, China

Siyu Chen
siyu_chen279@163.com
Zhejiang University
Hangzhou, Zhejiang
China

Cairong Zhao
zhaocairong@tongji.edu.cn
Tongji University
Shanghai, China

Longfei Liang
longfei.liang@neuhelium.com
NeuHelium Co., Ltd
Shanghai, China

Xiangyang Xue*
xyxue@fudan.edu.cn
Fudan University
Shanghai, China

Yanwei Fu*
yanweifu@fudan.edu.cn
Fudan University, Shanghai
Innovation Institute
Shanghai, China

Abstract

Open-vocabulary 3D visual grounding aims to localize target objects based on free-form language queries, which is crucial for embodied AI applications such as autonomous navigation, robotics, and augmented reality. Learning 3D language fields through neural representations enables accurate understanding of 3D scenes from limited viewpoints and facilitates the localization of target objects in complex environments. However, existing language field methods struggle to accurately localize instances using spatial relations in language queries, such as “the book on the chair.” This limitation mainly arises from inadequate reasoning about spatial relations in both language queries and 3D scenes. In this work, we propose **SpatialReasoner**, a novel neural representation-based framework with large language model (LLM)-driven spatial reasoning that constructs a visual properties-enhanced hierarchical feature field for open-vocabulary 3D visual grounding. To enable spatial reasoning in language queries, SpatialReasoner fine-tunes an LLM to capture spatial relations and explicitly infer instructions for the target, anchor, and spatial relation. To enable spatial reasoning in 3D scenes, SpatialReasoner incorporates visual properties (opacity and color) to construct a hierarchical feature field. This field represents language and instance features using distilled CLIP features and masks extracted via the Segment Anything Model (SAM). The field is then queried using the inferred instructions in a hierarchical manner to localize the target 3D instance based on the spatial relation in the language query. Notably, SpatialReasoner is not limited to a specific 3D neural representation; it serves as a framework adaptable to various representations, such as Neural Radiance Fields (NeRF) or 3D Gaussian Splatting (3DGS). Extensive experiments show that our framework can be seamlessly integrated into different neural representations, outperforming baseline models in 3D visual grounding while empowering their spatial reasoning capability. Project Homepage: [ZhenyangLiu.github.io/SpatialReasoner](https://github.com/ZhenyangLiu/SpatialReasoner).

CCS Concepts

• **Computing methodologies** → *Spatial and physical reasoning; Computer vision; Computer graphics.*

*Corresponding authors.

Keywords

Open-vocabulary 3D Visual Grounding, Spatial Reasoning, Visual Properties, Language Fields, Neural Representation

1 Introduction

Open-vocabulary 3D visual grounding [21, 28] aims to localize a target object in a 3D scene using free-form natural language descriptions, enabling humans to interact with the real world through open-ended language. Spatial reasoning is essential for this task, offering new opportunities for human-robot interaction [7, 33]. As shown in Figure 1, imagine a robot navigating a room and being asked, “Can you find the book that is on the chair?” The robot must interpret the spatial relationship between the book and the chair within the 3D environment, requiring both an understanding of the language and reasoning about spatial relations in real-time. This complex task demands that the robot not only comprehend language but also interprets spatial relations within both the language queries and the environment to precisely identify objects.

Recently, neural representations, such as Neural Radiance Fields (NeRF)[24] and 3D Gaussian Splatting (3DGS)[11], have emerged as powerful techniques for capturing complex scene structures from posed images. Recent advancements in neural representations have spurred extensive research on open-vocabulary 3D visual grounding with language fields [12, 29, 41]. LERF [12] introduces a novel approach to integrating language embeddings, extracted from 2D pretrained vision-language models such as CLIP [30], into NeRF-based 3D scene representations. LangSplat [29] employs 3DGS to build 3D neural representations and incorporates the semantic hierarchy from the Segment Anything Model (SAM) [14].

However, existing language field methods lack spatial reasoning capabilities, making it challenging to accurately localize target instances based on spatial relationships in language queries. As shown in Figure 1, regular language field methods localize objects directly based on complex user queries but fail to perceive spatial relationships in both the language query and the environment. Consequently, a localization error occurs: the *chair* is mislocalized, and the *book* specified by the user is not detected. This limitation mainly arises from inadequate reasoning about spatial relations in both language queries and 3D scenes: (1) **Lack of spatial reasoning**

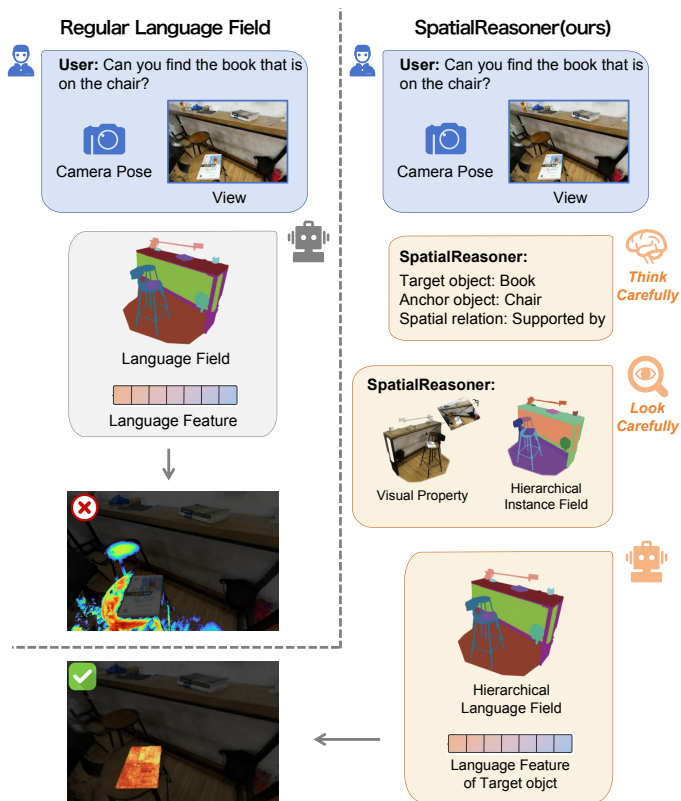


Figure 1: We propose *SpatialReasoner* for neural representation: prior language field methods localize instances directly from complex user queries but fail to capture spatial relations in both the language query and the environment (left). Our *SpatialReasoner* instead utilizes a large language model (LLM) and a hierarchical feature field to think and look “step by step” (right). Crucially, reasoning through an LLM—such as spatial relation decomposition—along with hierarchical language and instance fields, allows it to “think carefully” and “look carefully” before localizing the target instance.

within the language query. Existing language field methods employ the CLIP model for instruction comprehension. However, since the CLIP model is primarily trained on short texts, these methods struggle to accurately capture implicit spatial relations in complex language queries. (2) *Lack of spatial reasoning within the 3D scene.* Existing language field methods primarily focus on constructing language fields that capture object semantics alone. This limitation impairs spatial reasoning in 3D scenes, making it difficult to differentiate between objects that share the same concept.

In this work, we propose the *SpatialReasoner*, a novel neural representation-based framework with LLM-driven spatial reasoning that constructs a visual properties-enhanced hierarchical feature field for open-vocabulary 3D visual grounding. The *SpatialReasoner* incorporates spatial reasoning into both the 3D scene and language query, enabling accurate localization of specific instances based on the spatial relations described in the query. Figure 1 illustrates the process of spatial reasoning in our *SpatialReasoner*. The *SpatialReasoner* utilizes a large language model (LLM) and a hierarchical

feature field to think and look “step by step”. Crucially, reasoning through an LLM like spatial relation decomposition in addition to visual properties-enhanced hierarchical feature field to “think carefully” and “look carefully” before localizing the target instance.

Specifically, we fine-tune an LLM on the Sr3D and Sr3D++ [2] to enhance its reasoning capabilities, enabling decomposition of spatial relations in language instructions. The fine-tuned model parses complex queries into targets, anchors, and spatial relations. To facilitate 3D spatial reasoning, the *SpatialReasoner* incorporates visual attributes (opacity and color) to build a hierarchical feature field combining language and instance features. We first use SAM to extract 2D masks for all objects in the training dataset. The physical scales of objects are obtained by deprojecting the extracted masks into 3D space using depth information from scene reconstruction. *SpatialReasoner* incorporates visual properties derived from scene reconstruction using neural representations. The position and physical scale, along with the visual properties, are then used to construct a hierarchical feature field that includes both a language field and an instance field. Both fields are optimized with distilled CLIP features and extracted masks. The feature field is then queried hierarchically using the inferred instructions, activating potential target and anchor candidates. *SpatialReasoner* subsequently constructs an instance graph to further refine these candidates. Finally, by explicitly verifying whether the activated targets and anchors satisfy the spatial relationships, we precisely localize the specific 3D instance referenced in the language query. Notably, the proposed *SpatialReasoner* is not restricted to a specific 3D neural representation; it serves as a framework adaptable to various neural representations, such as NeRF and 3DGS.

To fully evaluate the effectiveness of *SpatialReasoner*, we conduct extensive experiments on the challenging LERF [12], Replica [34], and our newly developed Re3D datasets. To assess the generality of *SpatialReasoner*, we apply it to various 3D neural representations, including NeRF [24], Instant-NGP [25], and 3DGS [11]. We evaluate its performance in 3D visual grounding and spatial reasoning capabilities through comparative experiments on the LERF, Replica, and Re3D datasets, which include complex scenes with diverse objects that share identical semantics but distinct spatial relationships. Extensive experiments show that *SpatialReasoner* can be seamlessly integrated into various 3D neural representations. It not only outperforms baseline and previous state-of-the-art methods in 3D visual grounding but also achieves spatial reasoning beyond the capability of language field-based methods, accurately localizing specific instances based on spatial relations in language queries. The contributions of *SpatialReasoner* are summarized as follows:

- (1) **Empowering Language Field with Spatial Reasoning for 3D Visual Grounding:** We overcome the limitation of language field-based open-vocabulary 3D visual grounding, which struggles to localize instances using spatial relations in language queries, by introducing a visual properties-enhanced hierarchical feature field for robust spatial reasoning and accurate grounding.
- (2) **A Novel *SpatialReasoner* Framework:** The proposed *SpatialReasoner* leverages an LLM for spatial relation decomposition, alongside a visual properties-enhanced hierarchical feature field for spatial reasoning, to “think carefully” and

“look carefully”, enabling accurate step-by-step localization of target instances through explicit spatial reasoning.

- (3) **Outstanding Generality and Performance:** Extensive experiments demonstrate that our method can be seamlessly integrated into diverse 3D neural representations, outperforming baseline models in 3D visual grounding and empowering their spatial reasoning capabilities.

2 Related Work

Visual Grounding on 2D images. Visual grounding with natural language prompts is essential for robotics and augmented reality, with open-vocabulary localization being a major research focus. Datasets [15, 23, 39, 44] provide annotated image region descriptions. LSeg [16] uses a 2D image encoder to generate pixel-wise embeddings that align with CLIP text embeddings. CRIS [37] and CLIPSeg [22] create relevance maps from query CLIP embeddings. Some methods, like OpenSeg [6] and ViLD [8], predict masks and use CLIP for open-vocabulary classification. Unlike feature matching methods for visual grounding, our work focuses on the localization in 3D scenes with language queries.

Visual Grounding on 3D point clouds. Visual grounding on 3D point clouds has attracted growing interest due to its applications in 3D understanding and captioning [9, 10], autonomous driving [27], virtual reality [5], and notably robotic navigation and manipulation [18, 32]. Chen et al. [4] introduced the ScanRefer dataset and an end-to-end grounding-by-detection framework. ReferIt3D [2] proposed Nr3D and Sr3D datasets, differing by using ground-truth rather than predicted bounding boxes. InstanceRefer [40] employed a pretrained segmentation model with a handcrafted language parser to select candidate boxes. Nonetheless, these 3D point cloud methods heavily depend on extensive annotations and lack effective integration of 2D foundation model knowledge for zero-shot visual grounding.

3D Language Fields. Neural representations [11, 19, 24, 25, 36] have recently advanced scene reconstruction [31, 43] and novel view synthesis [26, 35]. Extending 2D foundation models across views, 3D language fields leverage CLIP features for open-vocabulary 3D visual grounding. Semantic-NeRF [36] integrates semantics into appearance and structure, while LERF [12] projects 2D CLIP embeddings into 3D via NeRF to construct language models within this framework. LangSplat [29] pioneered 3D Gaussian Splatting for language fields, and ReasonGrounder [20] exploits hierarchical 3D Gaussian features for visual grounding and reasoning. Nonetheless, these approaches struggle with precise instance localization due to inadequate spatial relation reasoning in language and 3D representations. In contrast, our SpatialReasoner employs a large language model (LLM) to decompose spatial relations and integrates visually enhanced hierarchical feature fields, enabling stepwise, accurate localization via spatial reasoning.

3 Method

As shown in Figure 2, we introduce SpatialReasoner, a neural representation-based framework that leverages an LLM for spatial relation decomposition in language queries, alongside visual properties-enhanced hierarchical feature fields for spatial reasoning and open-vocabulary 3D visual grounding.

3.1 Preliminary: Language Fields

To embed language features into spatial points within neural representations such as NeRF or 3DGS, language fields [12, 29] define a mapping function F that takes an input position and volume scale to generate the corresponding language embeddings. Given N calibrated input views with known pose information $\{I_i, P_i\}_{i=1}^N$, a 2D vision-language model extracts the corresponding ground-truth 2D features. Each expected pixel-wise language embedding ϕ_{lang} is obtained by casting a ray $\vec{x}(t) = \vec{o} + t\vec{d}$. The language field samples the initial volume scale $s(t)$ for each spatial point along the ray based on focal length and sampling distance from the ray origin. Using the same rendering weights as in volume rendering theory [3], defined as $T(t) = \int_s \exp(-\sigma(s))ds$ and $\omega(t) = \int_t T(t)\sigma(t)dt$, the expected pixel-wise language embedding ϕ_{lang} is computed as follows:

$$\begin{aligned}\hat{\phi}_{\text{lang}} &= \int_t \omega(t)F(\vec{x}(t), s(t))dt \\ \phi_{\text{lang}} &= \hat{\phi}_{\text{lang}} / \|\hat{\phi}_{\text{lang}}\|\end{aligned}\quad (1)$$

where $\hat{\phi}_{\text{lang}}$ denotes raw language rendering outputs, and ϕ_{lang} denotes the final normalized language embedding. This method combines 2D multimodal features to estimate pixel-level 2D representations, optimized by minimizing the loss between ϕ_{lang} and the 2D ground truth features.

During the querying stage, the language field computes the CLIP embedding of the language query, ϕ_{quer} , and the canonical phrases, ϕ_{canon}^i , to determine the appropriate volume scale for language embeddings. The relevance score R is then computed using Eqn. 2.

$$R = \min_i \frac{\exp(\phi_{\text{lang}} \cdot \phi_{\text{quer}})}{\exp(\phi_{\text{lang}} \cdot \phi_{\text{canon}}^i) + \exp(\phi_{\text{lang}} \cdot \phi_{\text{quer}})} \quad (2)$$

Language fields, commonly used in existing methods [12, 13, 29], is adopted by SpatialReasoner to lift 2D features into 3D within neural representations, enabling precise spatial reasoning and grounding.

3.2 Spatial Relation Decomposition

Given a language description, such as “Can you find the book that is on the chair?”, humans naturally decompose this description into distinct semantic directives, guiding us first to localize the “chair” (*anchor*), followed by transferring our focus from the “chair” to the “book” (*target*), facilitated by the intervening spatial relation “supported-by” (*spatial relation*). Inspired by this cognitive process, we introduce the LLM-driven method to “**think carefully**”: decomposing the given language description into a series of instructions denoted as $\{I_i\}_{i=1}^n$.

To enable spatial reasoning in language queries, we fine-tune large language models (LLMs) such as ChatGPT[1] to parse descriptions into key semantic components: the *anchor*, *target*, and their *spatial relation*. These parsed concepts are encoded into embeddings that serve as explicit instructions. This fine-tuning allows SpatialReasoner to accurately interpret and reason about implicit spatial relationships in complex queries. Moreover, the number of instructions (n) is adapted per benchmark; for instance, in Sr3D and Sr3D++[2], n is set to 3 to separately guide reasoning about the *target* category, *anchor* category, and their *spatial relation*. Further

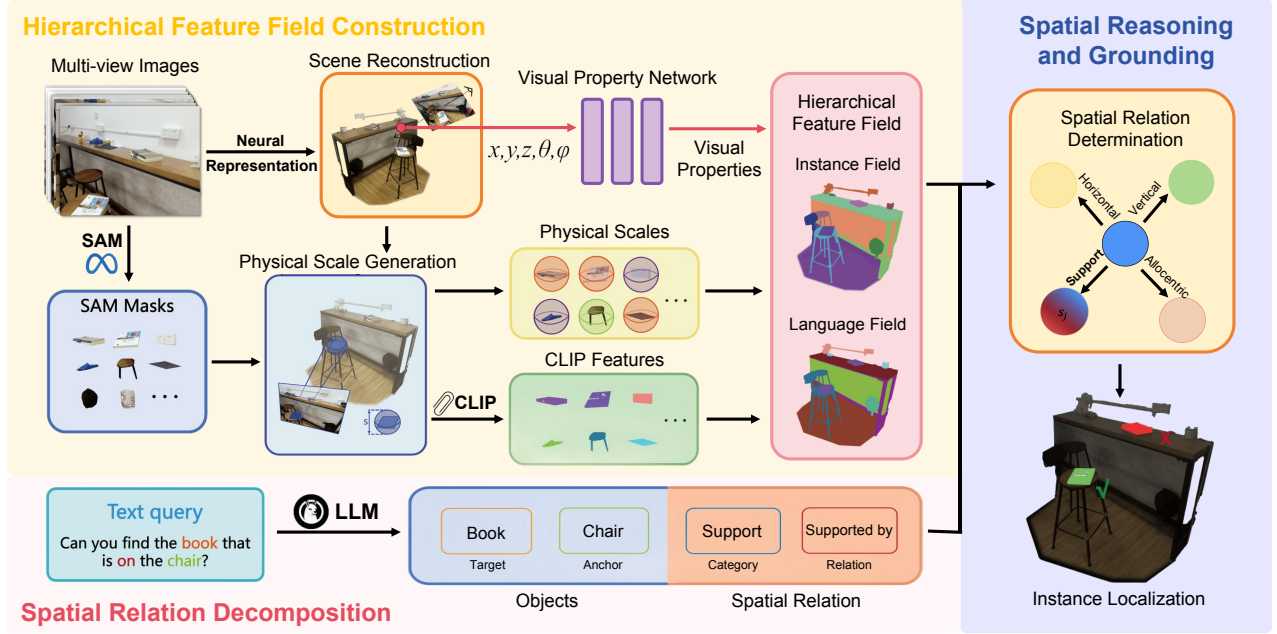


Figure 2: The overall pipeline of SpatialReasoner framework. SpatialReasoner fine-tunes an LLM to decompose language queries into targets, anchors, and spatial relations. It first employs SAM to generate 2D masks for diverse instances in the training dataset. Using a neural representation model (e.g., NeRF or 3DGS) trained on multi-view images, it obtains instance scales via depth depjection. By integrating visual properties (opacity and color) from scene reconstruction, SpatialReasoner constructs a hierarchical feature field that combines CLIP-extracted language features and mask-extracted instance features. Reasoned instructions then query these fields to identify target and anchor candidates. By analyzing spatial relations within the query and the 3D scene, SpatialReasoner precisely localizes the referenced 3D instance.

details on instruction generation are provided in the Supplementary Material.

3.3 Hierarchical Feature Field Construction

To enable spatial reasoning in 3D scenes and “look carefully”, SpatialReasoner integrates visual properties (opacity and color) to construct a hierarchical feature field that consists of both language and instance feature fields. Given the multi-view images, SpatialReasoner first trains a neural representation model (e.g., NeRF or 3DGS) to extract visual properties, calculate physical scales, and represent the geometric appearance within the hierarchical field. **Visual Property Extraction.** Existing language field methods encode language embeddings solely via spatial coordinates and volume scales, limiting their capacity to represent complex features such as blurred boundaries, visually similar objects, and transparent surfaces. This constraint impairs embedding quality and instance localization accuracy. Opacity and color at each spatial point provide rich geometric and appearance cues closely linked to language semantics. Opacity reflects material and structural properties, aiding classification, while color captures subtle visual details. By incorporating color into the language embedding, SpatialReasoner enhances discrimination of fine visual features, thereby improving accuracy and contextual understanding in 3D visual grounding. To enhance the quality of hierarchical features and improve the accuracy of 3D visual grounding, SpatialReasoner incorporates opacity and color as visual properties in the construction of the hierarchical

feature field. Based on the trained neural representation model, the opacity σ and color c can be extracted through the visual property network F_v , which takes in the 3D coordinate $\vec{x}(t)$ and the viewing direction (θ, ϕ) :

$$(\sigma, c) = F_v(\vec{x}(t), \theta, \phi). \quad (3)$$

SpatialReasoner relies on the neural representation to determine how to incorporate the visual properties (opacity and color) into the hierarchical feature field, including instance and language features. The construction of the two fields below illustrates these details.

Supervision Generation. SpatialReasoner first utilizes the automatic mask generator of SAM [14] to generate object masks from training views, which are then leveraged to assign physical scales and acquire pixel-aligned features. These masks are then filtered based on confidence, and nearly identical ones are deduplicated to generate mask candidates $\{M_1, M_2, \dots, M_n\}$. These candidates may overlap or encompass each other. Using the trained neural representation model, SpatialReasoner renders the depth of each mask’s pixels. Given the ray origin, the pixels of each mask can be deprojected onto 3D points using focal length and depth. By calculating the *standard deviation* of these points, we can estimate the physical scales $\{S_1, S_2, \dots, S_n\}$ for the objects. As a foundational multimodal model for text–vision interaction, CLIP [30] uses an image encoder to extract visual features and a text encoder to extract textual features. We then extract CLIP features $\{\phi_1, \phi_2, \dots, \phi_n\}$ for each segmented region across multiple training views to ensure

multi-view consistency. Thus, for each mask candidate, we obtain the associated triplet $\{M_i, S_i, \phi_i\}$.

Language Field. 3D visual grounding requires the model to localize a target object based on natural language queries. SpatialReasoner achieves this by constructing a language field within a hierarchical feature field. After obtaining the language embeddings ϕ_i and 3D physical scales S_i from 2D posed images, SpatialReasoner constructs a language field to model the relationships between 3D points and 2D pixels. Specifically, a ray $\vec{x}(t) = \vec{o} + t\vec{d}$ is cast from a pixel in the mask candidate M_k with physical scale S_k . SpatialReasoner incorporates the visual properties into the construction of language field. SpatialReasoner models a language field F_l that maps the input coordinate $\vec{x}(t)$, physical scale S_k , and visual properties $\{\sigma, c\}$ to the 3D language embeddings $F_l(\vec{x}(t), S_k, \sigma, c)$. It is important to note that $(\vec{x}(t), S_k) \in \mathbb{R}^{192}$ and $(\sigma, c) \in \mathbb{R}^4$, with the dimension of (σ, c) being much smaller than that of $(\vec{x}(t), S_k)$. Therefore, introducing density and color will not significantly increase the computational burden. Using the same rendering weights based on density σ as the neural representation, $w(t) = \int_t \exp(-\sigma(s))ds$, each expected pixel language feature $\hat{\phi}$ is rendered using $F_l(\vec{x}(t), S_k, \sigma, c)$:

$$\hat{\phi} = \int_t \omega(t) F_l(\vec{x}(t), S_k, \sigma, c) dt \quad (4)$$

where $F_l(\vec{x}(t), S_k, \sigma, c)$ denotes the language feature of spatial points on the ray. By optimizing the language loss $L_l = -\lambda_l \hat{\phi}_k \cdot \phi_k$, where λ_l is a hyperparameter, the language field learns to project 2D CLIP embeddings into 3D space.

Instance Field. The real world encompasses numerous complex scenarios, where instances sharing identical language features must be distinguished. For instance, while “book on the table” and “book on the chair” both involve the language feature “book”, they represent clearly distinct instances. To achieve this, SpatialReasoner constructs a hierarchical instance field to differentiate instances with identical language features and further refine localization precision. Similar to the language field, the instance field defines an instance mapping function F_{in} , which maps the input spatial coordinate $\vec{x}(t)$, physical scale S_k , and visual properties σ, c to the 3D instance embedding $F_{in}(\vec{x}(t), S_k, \sigma, c)$. These 3D instance embeddings can be rendered using the same rendering weights in neural representations, yielding the pixel instance feature ψ_k corresponding to the rays. The instance field is supervised using a margin-based contrastive objective. Specifically, two rays, r_i and r_j , are cast from the pixels in the masks M_i and M_j , with physical scales S_i and S_j . The instance features ψ_i and ψ_j are obtained by volumetrically rendering the embeddings along their respective rays r_i and r_j . The concrete contrastive loss L_{in} is formulated as:

$$L_{in} = \begin{cases} \|\psi_i - \psi_j\| & \text{if } M_i = M_j, \\ \text{ReLU}(\lambda_{in} - \|\psi_i - \psi_j\|) & \text{if } M_i \neq M_j, \end{cases} \quad (5)$$

where λ_{in} represents the bound constant as a hyperparameter. It is important to note that this instance loss is applied to rays sampled from the same viewpoint. This supervision allows the instance field to differentiate instances with identical language features and further enhance localization precision.

Analysis Opacity and color, as essential visual properties extracted from scene reconstruction, provide rich geometric and appearance

information that is effectively integrated into the hierarchical feature field construction. This enhances the quality of language embeddings, improving the accuracy of 3D visual grounding and spatial reasoning. Consequently, SpatialReasoner can effectively learn to represent high-quality language and instance features with complex characteristics. The effectiveness of the visual properties will be demonstrated in the experiments (Sec. 4).

SpatialReasoner is a versatile framework that constructs hierarchical feature fields using diverse neural representations, including Neural Radiance Fields (NeRF) for photorealistic scene modeling, Instant Neural Graphics Primitives (Instant-NGP) for fast training and rendering, and 3D Gaussian Splatting (3DGS) for efficient, scalable scene representation. This hierarchical construction enables SpatialReasoner to model 3D space through language-instance interactions, facilitating spatial reasoning and precise instance localization within complex 3D scenes.

3.4 Spatial Reasoning and Grounding

Through Spatial Relation Decomposition (“**think carefully**”) and Hierarchical Feature Field Construction (“**look carefully**”), SpatialReasoner has acquired spatial relationships embedded in complex text queries and a comprehensive scene representation, including geometry and appearance, language features, and instance features. Subsequently, SpatialReasoner will execute spatial reasoning and grounding to localize the target instance step-by-step.

Relevancy Map Activation. SpatialReasoner utilizes reasoned instructions from the finetuned LLM to hierarchically query the hierarchical feature field. Based on the reasoned target and anchor instructions, we first query the language field using spatial coordinates, physical scales, and visual properties. Consider that the physical scales $\{S_1, S_2, \dots, S_n\}$ of objects in 3D space and the CLIP embeddings $\{\phi_1, \phi_2, \dots, \phi_n\}$ are established during the supervision generation process. Additionally, the targets and anchors are bound to appear in the training images. To this end, the CLIP embeddings are used to compute the similarity with the CLIP textual features of the target and anchor instructions individually. The physical scales corresponding to the candidate with the highest similarity are used to query the language field and generate the language embedding maps. Thus, SpatialReasoner activates the relevance map through the similarity computation between the language embedding maps and the CLIP textual features of the target and anchor instructions.

Candidate Generation. Based on the relevance map, SpatialReasoner determines the relevant region candidates $\{C_1, C_2, \dots, C_n\}$ related to the language feature of target and anchor instructions, depending on the maximum relevance scores. To differentiate instances with similar language features and further refine localization precision, SpatialReasoner deprojects the relevant regions into 3D space for scale calculation and queries the hierarchical instance field for instance feature acquisition. SpatialReasoner deprojects the pixel with the maximum relevance from each relevant region to the 3D point and obtains the candidate instance feature.

Instance Graph Construction. Candidates determined based solely on language are often incomplete. We need to merge the candidates based on the instance feature. SpatialReasoner constructs the instance graph $G(V, E)$ to prune and merge the candidate set

$\{C_1, C_2, \dots, C_n\}$. The node set $V = \{v_1, v_2, \dots, v_n\}$ of the graph includes the features of the candidate objects. Next, we compute the affine differences A within the node set by measuring the Euclidean distances between node pairs:

$$A = \left\| V \otimes \mathbf{1}_n - (V \otimes \mathbf{1}_n)^T \right\|_2 \quad (6)$$

where $\mathbf{1}_n$ is a vector of all ones with size $n \times 1$ and \otimes denotes the tensor product. The edge set $E = \{e_{ij}\}$ is defined based on the differences A . Thus, $G(V, E)$ can be used to determine its connected components. The set of all connected components of the graph is denoted as $\{N_1, N_2, \dots, N_k\}$. Each connected component N_i merges the candidates into the final complete candidate \hat{C}_i using a bitwise OR operation:

$$\hat{C}_i = \vee_{j \in N_i} C_j \quad (7)$$

This step combines the candidates associated with each connected component into the final set of candidates $\{\hat{C}_1, \hat{C}_2, \dots, \hat{C}_k\}$. To localize specific instances from the candidates based on the reasoned spatial relation instructions, SpatialReasoner first determines the target and anchor candidates as described above. We deproject the target and anchor candidates into 3D space and warp them with bounding boxes. SpatialReasoner considers four spatial relations (Horizontal Proximity, Vertical Proximity, Support, Allocentric) to localize the specific instance. Generally, the language and instance fields are queried in a hierarchical manner based on the target and anchor instructions, and the specific object is determined accordingly with the spatial relation instructions. This enables SpatialReasoner to perform spatial reasoning and grounding within both 3D scenes and language queries, resulting in the accurate localization of specific instances mentioned in the language queries.

4 Experiments

4.1 Experimental Settings

Datasets. For quantitative and qualitative validation, we conduct experiments on the LERF [12] dataset, the Replica [34] dataset, and our developed Re3D dataset. Additionally, we fine-tune and evaluate an LLM on the Sr3D and Sr3D++ datasets [2].

- **LERF dataset.** The LERF dataset comprises real-world and posed long-tail scenes captured via the Polycam iPhone app, which employs on-board SLAM for camera pose estimation and feature extraction. SpatialReasoner utilizes an extended version of LERF with annotated ground truth, further augmented to evaluate 3D spatial reasoning and open-vocabulary visual grounding. To assess localization performance under spatial language queries, we enhance LERF by rendering novel views and generating ground truth labels using the Segment Anything Model (SAM).
- **Replica dataset.** The Replica dataset consists of high-quality reconstructions of various indoor spaces. Each reconstruction features clean, dense geometry, high-resolution, high-dynamic-range textures, glass and mirror surface information, planar segmentation, and semantic class and instance segmentation. Each scene is particularly well-suited for evaluating open-set 3D scene understanding.
- **Re3D dataset.** To further evaluate the capability of the proposed SpatialReasoner in localizing specific instances by

Table 1: Localization accuracy scores (%) on LERF dataset for spatial reasoning. The first three methods target 2D domain, whereas the remaining methods, including our SpatialReasoner, focus on 3D domain.

Method	<i>ramen</i>	<i>figurines</i>	<i>teatime</i>	<i>kitchen</i>	overall
LSeg [16]	11.4	12.2	10.4	10.6	11.2
ODISE [38]	12.1	21.8	23.6	21.3	19.7
OV-Seg [17]	21.5	22.1	23.8	20.4	21.9
LERF [12]	32.4	44.3	40.8	33.1	37.6
LangSplat [29]	45.4	31.2	58.7	48.8	46.1
SpatialReasoner(NeRF)	89.7	93.2	64.6	86.2	83.4
SpatialReasoner(NGP)	92.8	97.7	72.4	88.4	87.8
SpatialReasoner(3DGS)	94.1	98.3	83.2	91.5	91.7

understanding complex sentence queries containing spatial relations, we developed the Re3D dataset, which mainly involves various objects with the same semantics but differing spatial conditions. Similarly, the Re3D dataset is also captured using the Polycam, employing on-board SLAM.

Implementation Details. The Segment Anything Model [14] is used to generate the segmentation masks from the multi-view training images. The TinyLlama [42] model is used to comprehend the spatial relation within the language query to “think carefully”. The Adam optimizer with a weight decay of $1e-9$ is used for the proposal networks and fields. Training involves an exponential learning rate scheduler, transitioning from $1e-2$ to $1e-3$ during the first 5000 steps. All experiments are conducted on NVIDIA H100 GPUs.

Comparison Methods. Given the scarcity of existing methods for 3D spatial reasoning and grounding, we selected several representative approaches for comparison. Specifically, we compared our method with the following state-of-the-art methods: open-vocabulary 3D visual grounding methods LERF and LangSplat, and the open-vocabulary 2D semantic segmentation methods ODISE [38], OV-Seg [17], and LSeg [16]. To validate the generality of our SpatialReasoner, we further integrate the proposed SpatialReasoner into various neural representations: Neural Radiance Fields (NeRF), Instant-NGP (NGP), and 3D Gaussian Splatting (3DGS), which are denoted as **SpatialReasoner(NeRF)**, **SpatialReasoner(NGP)**, and **SpatialReasoner(3DGS)**, respectively.

Metrics. The experiments mainly utilize localization accuracy and mean intersection over union (mIoU) for evaluation. Localization accuracy considers a label a success if the highest relevance pixel falls inside the annotated box. The mIoU calculates the intersection ratio between the rendered relevance map and the annotated ground truth to measure the localization accuracy of the region.

4.2 Results of Spatial Reasoning

Quantitative Results. We compare our method with the comparison methods on the extended LERF, Replica, and Re3D datasets. As illustrated in Table 1 and Table 2, our method achieves an overall localization accuracy of 83.4%, 87.8%, and 91.7%, and an mIoU of 85.3%, 90.9%, and 92.8% by integrating SpatialReasoner into NeRF, Instant-NGP, and 3DGS, significantly outperforming the comparison methods. The Replica dataset is categorized into head, common, and tail based on the number of annotated points. As illustrated in

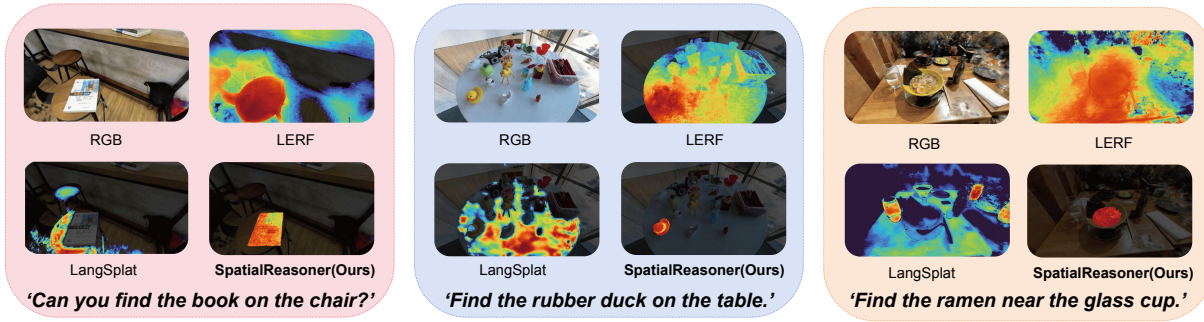


Figure 3: Qualitative comparisons of spatial reasoning capability. Results demonstrate that our SpatialReasoner achieves spatial reasoning and localizing the target instance based on the spatial relation.



Figure 4: Qualitative comparisons of 3D visual grounding capability. Results demonstrate that our SpatialReasoner achieves the superior accuracy in open-vocabulary 3D localization compared to other state-of-the-art methods.

Table 2: mIoU scores (%) on LERF dataset for spatial reasoning. The first three methods target 2D, whereas the remaining methods, including our SpatialReasoner, focus on 3D.

Method	<i>ramen</i>	<i>figurines</i>	<i>teatime</i>	<i>kitchen</i>	overall
LSeg [16]	14.4	16.0	19.2	24.5	18.5
ODISE [38]	22.4	14.1	22.5	28.4	21.8
OV-Seg [17]	33.2	18.9	21.4	26.4	24.9
LERF [12]	53.4	46.2	48.5	46.8	48.7
LangSplat [29]	58.5	59.2	54.4	63.2	58.8
SpatialReasoner(NeRF)	87.2	89.6	75.5	88.7	85.3
SpatialReasoner(NGP)	93.2	95.6	84.2	90.6	90.9
SpatialReasoner(3DGS)	93.6	97.4	86.5	93.7	92.8

Table 3: mIoU scores (%) on Replica dataset for spatial reasoning. The first three methods target 2D, whereas the remaining methods, including our SpatialReasoner, focus on 3D.

Methods	<i>head</i>	<i>common</i>	<i>tail</i>	overall
LSeg [16]	7.1	6.6	1.4	5.1
ODISE [38]	10.8	8.2	1.2	6.7
OV-Seg [17]	13.4	7.7	1.4	7.5
LERF [12]	19.2	10.1	2.3	10.5
LangSplat [29]	22.3	15.2	4.3	13.9
SpatialReasoner(NeRF)	22.8	16.7	6.2	15.2
SpatialReasoner(NGP)	26.5	28.3	10.2	21.6
SpatialReasoner(3DGS)	31.7	36.6	18.4	28.9

Table 3, our method outperforms the comparison methods across all categories. To further evaluate the capability for spatial reasoning, we compare our method with other methods on the Re3D dataset. Our method significantly improves the performance without significantly increasing the inference cost, as shown in Table 4.

Qualitative Results. Figure 3 illustrates the spatial reasoning results. SpatialReasoner demonstrates a robust spatial reasoning capability, enabling it to localize instances based on the spatial relations in language queries. It provides accurate 3D localization even in complex real-world scenes. For instance, given the query “Can you find the book on the chair?” SpatialReasoner accurately

localizes the book on the chair, whereas LERF and LangSplat fail to handle this query involving spatial reasoning.

4.3 Results of Grounding

Quantitative Results. SpatialReasoner can be integrated into different neural representations, outperforming existing methods on 3D visual grounding. As demonstrated in Table.5, our method achieves an overall localization accuracy of 70.2%, 75.0%, and 79.9% by integrating SpatialReasoner into NeRF, Instant-NGP, and 3DGS, significantly outperforming the comparison methods.

Table 4: Quantitative results on Re3D dataset for spatial reasoning. Acc denotes the localization accuracy, mIoU denotes the mean IoU score, and Speed denotes the activation time for a single view.

Methods	Acc(%)	mIoU(%)	Speed(s)
LSeg [16]	24.1	18.6	1.43
ODISE [38]	32.4	33.6	1.22
OV-Seg [17]	38.4	34.8	1.23
LERF [12]	71.4	44.6	0.93
LangSplat [29]	85.6	51.2	0.04
SpatialReasoner(NeRF)	85.8	52.4	1.43
SpatialReasoner(NGP)	91.4	62.6	0.44
SpatialReasoner(3DGS)	92.6	64.8	0.08

Table 5: Localization accuracy scores on extended LERF dataset (LERF-ex), Re3D dataset, and Replica dataset for spatial reasoning. The first three methods target 2D domain, whereas the remaining methods, including our SpatialReasoner, focus on 3D domain.

Methods	LERF-ex	Re3D	Replica	overall
LSeg [16]	21.6	34.8	17.2	24.5
ODISE [38]	30.2	43.8	28.6	34.2
OV-Seg [17]	35.4	52.6	30.2	39.4
LERF [12]	74.8	45.4	32.2	50.8
LangSplat [29]	85.4	56.3	42.6	61.4
SpatialReasoner(NeRF)	91.8	67.6	51.2	70.2
SpatialReasoner(NGP)	93.2	72.4	59.4	75.0
SpatialReasoner(3DGS)	94.5	76.8	68.4	79.9

Table 6: Ablation studies of key components on LERF dataset. We report the mIoU score (%) for performance evaluation and inference time (s) for computation cost evaluation.

Component		Performance (mIoU / Inference Time)	
VP	HIF	IG	3D Visual Grounding / Spatial Reasoning
			78.2/0.038 / ✗
✓			82.4/0.042 / ✗
✓	✓		88.3/0.051 / 86.9/0.072
✓	✓	✓	94.5/0.063 / 91.7/0.091

Qualitative Results. We show the high quality of open-vocabulary 3D visual grounding in SpatialReasoner compared to other methods in challenging and realistic scenes. Figure 4 illustrates the visual results of this comparison. We note that the activation areas generated by other methods are often more scattered, while our approach yields more accurate regions.

4.4 Ablation Study

Ablations are conducted on the LERF dataset with SpatialReasoner(3DGS) in Table 6. Without the proposed components, we only

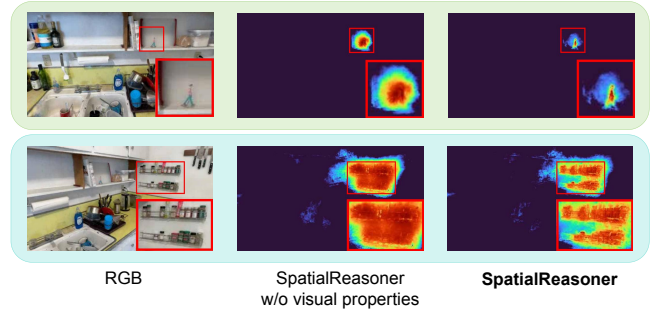


Figure 5: Ablation Study on visual properties with qualitative degradation examples.



Figure 6: Ablation Study on instance graph construction with qualitative degradation examples.

utilize the hierarchical language field to enable open-vocabulary 3D visual grounding. It achieves a mIoU score of 78.2% and renders each view in 0.038 seconds. Through the introduction of visual properties (VP) from scene reconstruction, SpatialReasoner further enhance the performance of 3D visual grounding by 4.2%. Furthermore, SpatialReasoner introduces a hierarchical instance field (HIF) for spatial reasoning, enabling 3D localization with spatial relations. By incorporating the instance graph construction (IG), SpatialReasoner further increases the performance of grounding by 6.2% and spatial reasoning by 4.6%. We also provide qualitative comparison results in Figure 5 and Figure 6.

5 Conclusion

We propose a novel neural representation-based framework with LLM-driven spatial reasoning, SpatialReasoner, for open-vocabulary 3D visual grounding. SpatialReasoner leverages an LLM for spatial relation decomposition, along with visual property-enhanced hierarchical feature fields for spatial reasoning, allowing it to “think carefully” and “look carefully,” enabling accurate, step-by-step localization of the target instance. Extensive experiments demonstrate that our method can be seamlessly integrated into various 3D neural representations, surpassing baseline models in 3D visual grounding and empowering their spatial reasoning capabilities.

6 Acknowledgments

This work was supported in part by NSFC Project (62176061), Science and Technology Commission of Shanghai Municipality (No.24511103100), Doubao Fund, and Shanghai Technology Development and Entrepreneurship Platform for Neuromorphic and AI SoC. The authors gratefully acknowledge the support and resources provided by these organizations

References

- [1] Josh Achiam, Steven Adler, Sandhini Agarwal, Lama Ahmad, Ilge Akkaya, Florencia Leoni Aleman, Diogo Almeida, Janko Altenschmidt, Sam Altman, Shyamal Anadkat, et al. 2023. Gpt-4 technical report. *arXiv preprint arXiv:2303.08774* (2023).
- [2] Panos Achlioptas, Ahmed Abdelreheem, Fei Xia, Mohamed Elhoseiny, and Leonidas Guibas. 2020. Referit3d: Neural listeners for fine-grained 3d object identification in real-world scenes. In *Computer Vision—ECCV 2020: 16th European Conference, Glasgow, UK, August 23–28, 2020, Proceedings, Part I 16*. Springer, 422–440.
- [3] Robert A Brebin, Loren Carpenter, and Pat Hanrahan. 1998. Volume rendering. In *Seminal graphics: pioneering efforts that shaped the field*. 363–372.
- [4] Dave Zhenyu Chen, Angel X Chang, and Matthias Nießner. 2020. Scanrefer: 3d object localization in rgb-d scans using natural language. In *European conference on computer vision*. Springer, 202–221.
- [5] Nianchen Deng, Zhenyi He, Jiannan Ye, Budmonde Duinkharjav, Praneeth Chakravarthula, Xubo Yang, and Qi Sun. 2022. Fov-nerf: Foveated neural radiance fields for virtual reality. *IEEE Transactions on Visualization and Computer Graphics* 28, 11 (2022), 3854–3864.
- [6] Golnaz Ghiasi, Xiuye Gu, Yin Cui, and Tsung-Yi Lin. 2022. Scaling open-vocabulary image segmentation with image-level labels. In *European Conference on Computer Vision*. Springer, 540–557.
- [7] Michael A Goodrich, Alan C Schultz, et al. 2008. Human–robot interaction: a survey. *Foundations and Trends® in Human–Computer Interaction* 1, 3 (2008), 203–275.
- [8] Xiuye Gu, Tsung-Yi Lin, Weicheng Kuo, and Yin Cui. 2021. Open-vocabulary object detection via vision and language knowledge distillation. *arXiv preprint arXiv:2104.13921* (2021).
- [9] Huy Ha and Shuran Song. 2022. Semantic abstraction: Open-world 3d scene understanding from 2d vision-language models. *arXiv preprint arXiv:2207.11514* (2022).
- [10] Yining Hong, Haoyu Zhen, Peihao Chen, Shuhong Zheng, Yilun Du, Zhenfang Chen, and Chuang Gan. 2023. 3d-llm: Injecting the 3d world into large language models. *Advances in Neural Information Processing Systems* 36 (2023), 20482–20494.
- [11] Bernhard Kerbl, Georgios Kopanas, Thomas Leimkühler, and George Drettakis. 2023. 3d gaussian splatting for real-time radiance field rendering. *ACM Transactions on Graphics* 42, 4 (2023), 1–14.
- [12] Justin Kerr, Chung Min Kim, Ken Goldberg, Angjoo Kanazawa, and Matthew Tancik. 2023. Lrf: Language embedded radiance fields. In *Proceedings of the IEEE/CVF International Conference on Computer Vision*. 19729–19739.
- [13] Chung Min Kim, Mingxuan Wu, Justin Kerr, Ken Goldberg, Matthew Tancik, and Angjoo Kanazawa. 2024. GARField: Group Anything with Radiance Fields. *arXiv preprint arXiv:2401.09419* (2024).
- [14] Alexander Kirillov, Eric Mintun, Nikhila Ravi, Hanzi Mao, Chloe Rolland, Laura Gustafson, Tete Xiao, Spencer Whitehead, Alexander C Berg, Wan-Yen Lo, et al. 2023. Segment anything. In *Proceedings of the IEEE/CVF International Conference on Computer Vision*. 4015–4026.
- [15] Ranjay Krishna, Yuke Zhu, Oliver Groth, Justin Johnson, Kenji Hata, Joshua Kravitz, Stephanie Chen, Yannis Kalantidis, Li-Jia Li, David A Shamma, et al. 2017. Visual genome: Connecting language and vision using crowdsourced dense image annotations. *International journal of computer vision* 123 (2017), 32–73.
- [16] Boyi Li, Kilian Q Weinberger, Serge Belongie, Vladlen Koltun, and René Ranftl. 2022. Language-driven semantic segmentation. *arXiv preprint arXiv:2201.03546* (2022).
- [17] Feng Liang, Bichen Wu, Xiaoliang Dai, Kumpeng Li, Yanan Zhao, Hang Zhang, Peizhao Zhang, Peter Vajda, and Diana Marculescu. 2023. Open-vocabulary semantic segmentation with mask-adapted clip. In *Proceedings of the IEEE/CVF Conference on Computer Vision and Pattern Recognition*. 7061–7070.
- [18] Haitao Lin, Yanwei Fu, and Xiangyang Xue. 2023. PourIt!: Weakly-supervised Liquid Perception from a Single Image for Visual Closed-Loop Robotic Pouring. In *Proceedings of the IEEE/CVF International Conference on Computer Vision*. 241–251.
- [19] Yichen Liu, Benran Hu, Junkai Huang, Yu-Wing Tai, and Chi-Keung Tang. 2023. Instance neural radiance field. In *Proceedings of the IEEE/CVF International Conference on Computer Vision*. 787–796.
- [20] Zhenyang Liu, Yikai Wang, Sixiao Zheng, Tongying Pan, Longfei Liang, Yanwei Fu, and Xiangyang Xue. 2025. ReasonGrounder: LVLm-Guided Hierarchical Feature Splatting for Open-Vocabulary 3D Visual Grounding and Reasoning. *arXiv preprint arXiv:2503.23297* (2025).
- [21] Shiyang Lu, Haonan Chang, Eric Pu Jing, Abdeslam Boularias, and Kostas Bekris. 2023. Ovir-3d: Open-vocabulary 3d instance retrieval without training on 3d data. In *Conference on Robot Learning*. PMLR, 1610–1620.
- [22] Timo Lüddecke and Alexander Ecker. 2022. Image segmentation using text and image prompts. In *Proceedings of the IEEE/CVF conference on computer vision and pattern recognition*. 7086–7096.
- [23] Junhua Mao, Jonathan Huang, Alexander Toshev, Oana Camburu, Alan L Yuille, and Kevin Murphy. 2016. Generation and comprehension of unambiguous object descriptions. In *Proceedings of the IEEE conference on computer vision and pattern recognition*. 11–20.
- [24] Ben Mildenhall, Pratul P Srinivasan, Matthew Tancik, Jonathan T Barron, Ravi Ramamoorthi, and Ren Ng. 2021. Nerf: Representing scenes as neural radiance fields for view synthesis. *Commun. ACM* 65, 1 (2021), 99–106.
- [25] Thomas Müller, Alex Evans, Christoph Schied, and Alexander Keller. 2022. Instant neural graphics primitives with a multiresolution hash encoding. *ACM transactions on graphics (TOG)* 41, 4 (2022), 1–15.
- [26] Simon Niedermayr, Josef Stumpfeffer, and Rüdiger Westermann. 2024. Compressed 3d gaussian splatting for accelerated novel view synthesis. In *Proceedings of the IEEE/CVF Conference on Computer Vision and Pattern Recognition*. 10349–10358.
- [27] Jelena Novosel, Prashanth Viswanath, and Bruno Arsenali. 2019. Boosting semantic segmentation with multi-task self-supervised learning for autonomous driving applications. In *Proc. of NeurIPS-Workshops*, Vol. 3.
- [28] Songyou Peng, Kyle Genova, Chiyu Jiang, Andrea Tagliasacchi, Marc Pollefeys, Thomas Funkhouser, et al. 2023. Openscene: 3d scene understanding with open vocabularies. In *Proceedings of the IEEE/CVF Conference on Computer Vision and Pattern Recognition*. 815–824.
- [29] Minghan Qin, Wanhua Li, Jiawei Zhou, Haoqian Wang, and Hanspeter Pfister. 2023. LangSplat: 3D Language Gaussian Splatting. *arXiv preprint arXiv:2312.16084* (2023).
- [30] Alec Radford, Jong Wook Kim, Chris Hallacy, Aditya Ramesh, Gabriel Goh, Sandhini Agarwal, Girish Sastry, Amanda Askell, Pamela Mishkin, Jack Clark, et al. 2021. Learning transferable visual models from natural language supervision. In *International conference on machine learning*. PMLR, 8748–8763.
- [31] Fabio Remondino, Ali Karami, Ziyang Yan, Gabriele Mazzacca, Simone Rigon, and Rongjun Qin. 2023. A critical analysis of NeRF-based 3D reconstruction. *Remote Sensing* 15, 14 (2023), 3585.
- [32] Dhruv Shah, Benjamin Eysenbach, Gregory Kahn, Nicholas Rhinehart, and Sergey Levine. 2021. Ving: Learning open-world navigation with visual goals. In *2021 IEEE International Conference on Robotics and Automation (ICRA)*. IEEE, 13215–13222.
- [33] Thomas B Sheridan. 2016. Human–robot interaction: status and challenges. *Human factors* 58, 4 (2016), 525–532.
- [34] Julian Straub, Thomas Whelan, Lingni Ma, Yufan Chen, Erik Wijmans, Simon Green, Jakob J Engel, Raul Mur-Artal, Carl Ren, Shobhit Verma, et al. 2019. The replica dataset: A digital replica of indoor spaces. *arXiv preprint arXiv:1906.05797* (2019).
- [35] Matthew Tancik, Vincent Casser, Xinchun Yan, Sabeek Pradhan, Ben Mildenhall, Pratul P Srinivasan, Jonathan T Barron, and Henrik Kretschmar. 2022. Block-nerf: Scalable large scene neural view synthesis. In *Proceedings of the IEEE/CVF conference on computer vision and pattern recognition*. 8248–8258.
- [36] Suhani Vora, Noha Radwan, Klaus Greff, Henning Meyer, Kyle Genova, Mehdi SM Sajadi, Etienne Pot, Andrea Tagliasacchi, and Daniel Duckworth. 2021. Nesf: Neural semantic fields for generalizable semantic segmentation of 3d scenes. *arXiv preprint arXiv:2111.13260* (2021).
- [37] Zhaoping Wang, Yu Lu, Qiang Li, Xunqiang Tao, Yandong Guo, Mingming Gong, and Tongliang Liu. 2022. Cris: Clip-driven referring image segmentation. In *Proceedings of the IEEE/CVF conference on computer vision and pattern recognition*. 11686–11695.
- [38] Jiarui Xu, Sifei Liu, Arash Vahdat, Wonmin Byeon, Xiaolong Wang, and Shalini De Mello. 2023. Open-vocabulary panoptic segmentation with text-to-image diffusion models. In *Proceedings of the IEEE/CVF Conference on Computer Vision and Pattern Recognition*. 2955–2966.
- [39] Licheng Yu, Patrick Poisson, Shan Yang, Alexander C Berg, and Tamara L Berg. 2016. Modeling context in referring expressions. In *Computer Vision—ECCV 2016: 14th European Conference, Amsterdam, The Netherlands, October 11–14, 2016, Proceedings, Part II 14*. Springer, 69–85.
- [40] Zhihao Yuan, Xu Yan, Yinghong Liao, Ruimao Zhang, Sheng Wang, Zhen Li, and Shuguang Cui. 2021. Instancerefer: Cooperative holistic understanding for visual grounding on point clouds through instance multi-level contextual referring. In *Proceedings of the IEEE/CVF International Conference on Computer Vision*. 1791–1800.
- [41] Hao Zhang, Fang Li, and Narendra Ahuja. 2024. Open-NeRF: Towards Open Vocabulary NeRF Decomposition. In *Proceedings of the IEEE/CVF Winter Conference on Applications of Computer Vision*. 3456–3465.
- [42] Peiyuan Zhang, Guangtao Zeng, Tianduo Wang, and Wei Lu. 2024. Tinyllama: An open-source small language model. *arXiv preprint arXiv:2401.02385* (2024).
- [43] Xiaoshuai Zhang, Sai Bi, Kalyan Sunkavalli, Hao Su, and Zexiang Xu. 2022. Nerfusion: Fusing radiance fields for large-scale scene reconstruction. In *Proceedings of the IEEE/CVF Conference on Computer Vision and Pattern Recognition*. 5449–5458.
- [44] Luowei Zhou, Yannis Kalantidis, Xinlei Chen, Jason J Corso, and Marcus Rohrbach. 2019. Grounded video description. In *Proceedings of the IEEE/CVF conference on computer vision and pattern recognition*. 6578–6587.